MODELLING OF RE-ENTRY FLOWS: EXPERTISE AVAILABLE AT ISA

Philippe Reynier

Ingénierie et Systèmes Avancés, Technopole Bordeaux Technowest, 19 allée James Watt, 33700 Mérignac, France, Email:Philippe.Reynier@isa-space.eu

ABSTRACT

The present contribution focuses on the means, in term of software, and expertise on modelling, related to re-entry flows available at ISA. Using the in-house software a large number of phenomena related to re-entry can be numerically investigated. Moreover, a significant experience is already available in several areas: trajectories, transition to turbulence, blackout, CFD, radiation, and ablation.

1. INTRODUCTION

The purpose of this contribution is to present the tools and the experience on re-entry aerothermodynamics available at Ingénierie et Systèmes Avancés (ISA). The majority of the in-house tools are available through a cooperation with Fluid Gravity Engineering. The results show here, on different problems related to re-entry: ablation, blackout, CFD, radiation, trajectory analysis and transition to turbulence gather some elements of different studies performed at ESA-ESTEC in re-entry on several projects and programmes such as ATV, AURORA, EURORETURN, IRDT, PARES, JEP, EXOMARS, HUYGENS, INTERMARSNET and SCIROCCO. Some of these activities have actually a continuity at ISA with some on-going works performed in the domains of ablation and blackout.

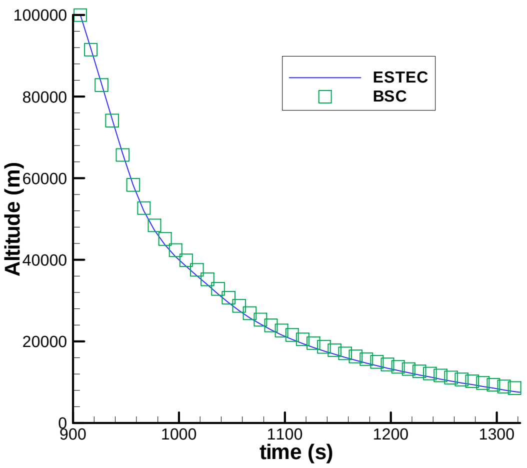

Figure 1: Trajectories of IRDT re-entry predicted by Babakin Space Center (BSC) and ESTEC.

2. TRAJECTORY ANALYSIS

Several tools are available for the trajectory analysis: TRAJ3D [1], TRAJ6D [2] and CREAM [3]. The first one is a three degree of freedom trajectory code used for the parametric studies of planetary entries. Different planet atmospheres (Earth, Titan, Mars) are integrated, there is a possibility of parachute opening, the entry can be ballistic or not (a lift can be taken into account, and the rarefied effects are accounted for. This tool computes also the stagnation heat-flux using correlations and a first assessment of ablation recession can be performed. TRAJ6D is a six degree of freedom trajectory code computing the complete dynamic motion of a body in a planetary gravity field with or without an atmosphere (wind models are incorporated). A Monte Carlo capability and specific guidance algorithms are incorporated. The last tool, CREAM [3] is a recent coupled method for reentry based on the coupling between a boundary layer code RKHMP [4], TRAJ6D and a viewer.

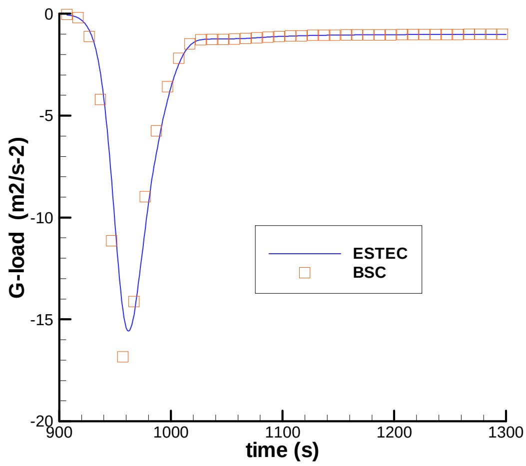

Figure 2: G-load distributions along IRDT trajectory predicted by BSC and ESTEC.

The trajectory codes have been extensively used at ESTEC in the frame of several projects. Among them we can cite IRDT for the mission analysis [5], the preparation of post flight and the post flight analysis [6]. For the mission analysis the results obtained with TRAJ3D have been compared with those of the Babakin Space Center (BSC) [7]. Both predictions of

ESTEC and BSC are displayed in Figures 1 and 2 for the distributions of altitude and g-load along the trajectory respectively. There is generally a good agreement with some slight difference (around 8%) for the maximum of g-load that might be due to a different atmosphere model used by BSC. The same tools have also been used for the prediction of the destructive re-entry of ATV [8] and to rebuild the re-entry trajectory of PARES [9].

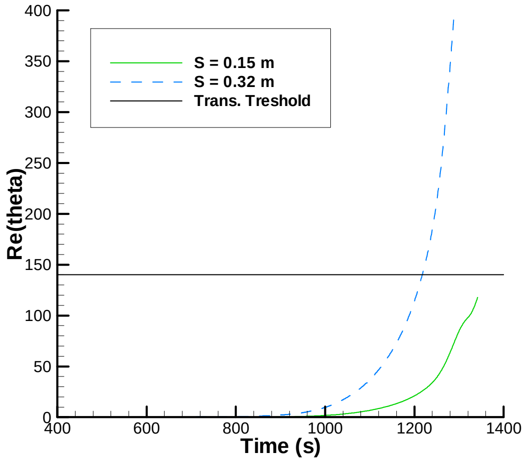

Figure 3: Evolution of the transition criterion, Re_θ, during PARES entry. The horizontal line is the transition threshold and S the curvilinear coordinate.

3. TRANSITION TO TURBULENCE

For preliminary studies, the occurrence of transition to turbulence is assessed along the trajectory using engineering correlations integrated in the trajectory codes. An extensive review of the different existing correlations has been performed in the early eighties [10] and comparisons with both wind-tunnels and flight experiments performed. Recently [11], a survey of these different criteria has been performed in order to assess their applicability for the entry of blunt bodies. The conclusion of the survey was to use Re_θ (where is the θ boundary layer thickness) to assess the transition over a smooth surface. For blunt entry vehicles, the value of Re_θ for transition determination found in the literature varies between 140 and 250. This value of 140 has been selected for the assessment of transition along PARES trajectory. The values of Re_θ for two locations of the geometry are displayed in Figure 3. They show that transition will most likely occur at the shoulder of the capsule (location S=0.32 m) during its reentry.

During re-entry with an ablative material the transition is driven by surface microroughness. The roughness produces disturbances within the laminar boundary layer. When the altitude decreases, the Reynolds number increases, and the flow conditions capable of amplifying these roughness-induced disturbances are eventually achieved. The problem is to quantify the disturbance generation capability of a given surface roughness.

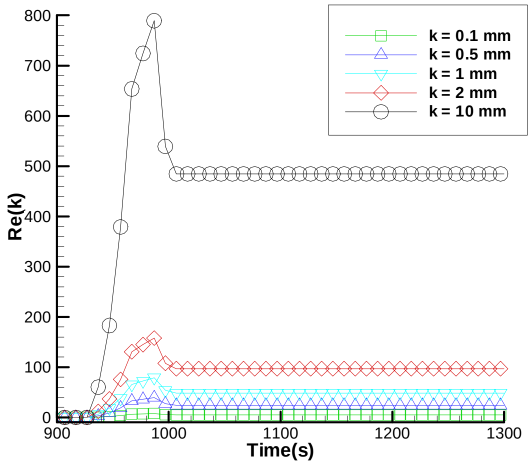

Figure 4: Distribution of the roughness height Reynolds number Re_k during IRDT entry, for different values of the roughness, k.

The recommendation of the review [11] was to use the correlation proposed by Reda [10] for roughness-dominated transition. This criterion is given by,

$$\mathrm{Re}_k = \left[\frac{\rho_e U_e k}{\mu_e}\right]_{TR} \cong 106 \qquad (1)$$

where ρ_e, U_e and μ_e are the density, the velocity and the dynamic viscosity at the boundary layer edge respectively. Re_k is the roughness height Reynolds number, Re_k, The critical value of Re_k is 106 with an uncertainty of 20%.

Since the thermal protection system of IRDT was made of an ablative material, the transition along the capsule re-entry path has been checked using this last correlation. The distribution of the roughness height Reynolds number, Re_k, computed for different roughness values of the shield is plotted in Figure 4. The results show that for a boundary edge of 1 mm, the critical threshold for transition is reached. This value of 1mm is much smaller than the two steps present along IRDT geometry: one of 41 mm between the front shield and the cone and the second of 10 mm at the junction with the inflatable part. As shown in Figure 4, these two steps increase drastically the transition possibilities upstream of the capsule. The predictions show very high levels of Re_k already in the early stages of the entry. The fact that there are two successive steps is also in favour of the turbulence development. If the transition happens at the first gap, located at the border of the front shield, the boundary layer will be already turbulent upstream of the second step and the flow could be fully turbulent over the complete capsule. The consequences of a flow transition to turbulence are higher drag, heat-flux and shear stress. Hence, the capsule has been designed accounting for a turbulent heat-flux and a thicker thermal protection system has been considered to account for turbulence effects.

4. BLACKOUT

During the re-entry in a planet atmosphere, communication blackout may occur. This phenomenon is induced by the electronic density surrounding the vehicle and depends on the level of ionisation. As a consequence, blackout duration depends on several parameters such as the entry conditions, the planet atmosphere and the antenna frequency band. When the critical density of electrons for the antenna frequency band is reached, communications are cut. An engineering method has been developed at ESTEC [5] to evaluate blackout duration. The critical electron density is determined as in [12]. For a given electron density, n_e, the corresponding plasma frequency, f_p, in Hz, is expressed as,

$$f_p = \tfrac{1}{2\pi}\sqrt{\frac{q^2 n_e}{\varepsilon_0 m_e}} \tag{2}$$

where q is the electron charge, m_e the electron mass and ε_0 the permittivity of vacuum. From this equation the critical density, $n_{e,crit}$, for a communication antenna is given as,

$$n_{e,crit} = \frac{{f_{ant}}^2}{80.64\,.\,10^6} \tag{3}$$

where f_{ant} is the antenna frequency, expressed in Hz.

For determining the electron density around the capsule, the shock layer is investigated with PMSSR [13] that is a solver based on an inverse method. This tool does not require a lot of computational effort and a complete trajectory path can be easily investigated. Using this tool the electron density within the shock layer can be determined and compared to the critical density.

Using this technique, the blackout duration has been estimated for an Earth aerocapture [14] and for the IRDT mission [7]. For an Earth aerocapture the blackout is found to be very long: 120 s for a Ka-band antenna, 180 s for the X-band, and nearly all the manoeuvre, 230 s, for the S-band. The results predicted here are close to those obtained at NASA using a similar approach [12] (but coupled to a CFD solver) for a similar manoeuvre, has predicted a blackout duration of 280 s for S-band, 130 s for X-band and no blackout for Ka-band. For Apollo re-entry, which was not direct, the blackout duration was lasting several minutes. Although Apollo was ablative, pure air chemistry was dominating the plasma composition at the high velocities [15].

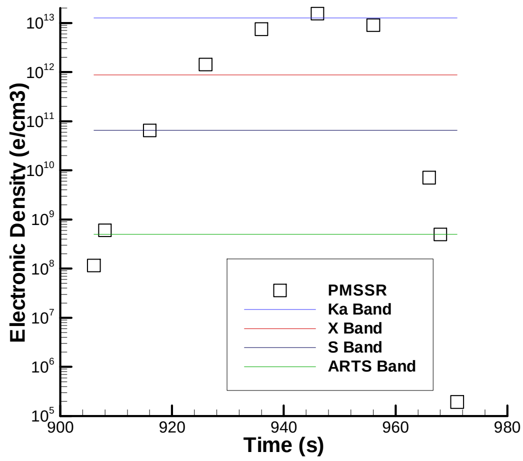

Figure 5: Evolution of the electronic density during IRDT entry. The horizontal lines correspond to the critical density for Ka, X, S and ARTS bands.

The same investigation has been performed for IRDT mission. During the flight, an Autonomous Radio Telemetry System (ARTS) ensures the communications with the ground. The antenna is embedded in the heat-shield and emits forward. The electronic density at the stagnation point along the trajectory has been computed and compared to the ARTS critical electronic density. The results are reported in Figure 5 and shows that the blackout period starts at t = 906,94 s and lasts 60 s. BSC has performed the same work [7] and the blackout zone is also estimated at 60 s in their prediction.

As a consequence the engineering technique used here is able to provide a first estimate of the blackout period. The method can be refined with a sensibility study on the thermochemical models and a comparison with CFD computations for predicting the electronic density. The present analysis neglects the ablation process that can create species increasing the level of ionisation. For a more deep study, predictions with coupling between CFD and electromagnetic computations are required. An on-going activity for the post flight analysis of IRDT mission has been started and the blackout predictions will be carried through coupling between a CFD code and a solver of the Maxwell equations.

5. CFD

For the flow-field prediction, engineering tools and CFD codes are available: PMSSR [13] for the shock layer analysis, RKHMP [4] a boundary layer code for heat-flux calculations, and TINA [16] a 3D finite-volume code for Navier-Stokes predictions. TINA accounts for chemical and thermal non equilibrium, catalysis, ablation, turbulence and can be coupled with PARADE [17-18] for radiation analysis. Other Navier-

Stokes codes devoted to compressible and incompressible flows are also available.

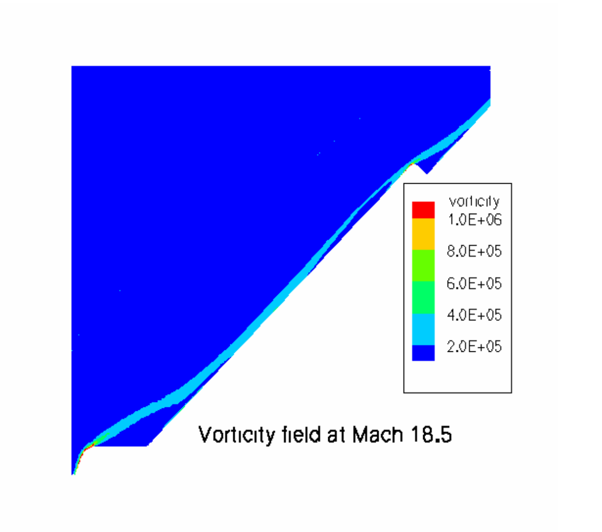

Figure 6: Vorticity field at Mach 18.5 over the IRDT cone [5].

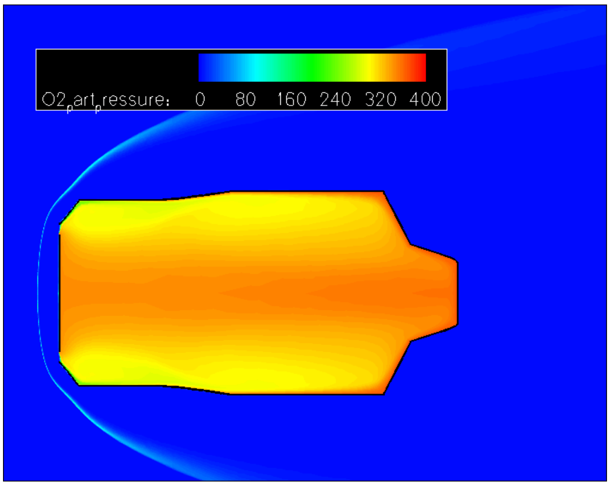

Figure 7: Flow-field of diatomic oxygen inside and outside the ATV in presence of a fissure.

The experience in CFD available in-house is significant, it has been acquired in several European research institutes (DLR, ESTEC, IMFT) for wide range of applications [19]. Today, CFD has reached a high maturity and can be applied to a wide range of aerothermodynamics and propulsion problems. In the perspective of re-entry, CFD solvers can be used for different tasks.

One of the first usefulness of CFD is to support the preliminary predictions obtained using engineering codes. This is demonstrated in Figures 6 and 7. Figure 6 represents the vorticity field over the IRDT cone simulated with the DLR TAU [20] code. This numerical simulation has been performed to precise the boundary layer behaviour at the two steps located over the cone. The presence of two backward facing steps, visible in ***Figure 6***, induces locally a complicated flow pattern with the presence of separated regions, shear-layers and shock/boundary layer interactions. The figure shows a succession or three laminar separated areas which have a destabilizing effect on the boundary layer. The laminar separation is an unsteady phenomenon which is strongly linked to the transition to turbulence [21-22]. When the instability is amplified, a three-dimensional bifurcation can occur, leading to a transitional flow [23]. The flow-field of vorticity simulated here reinforces the assessment of transition to turbulence performed with empirical correlations in §3.

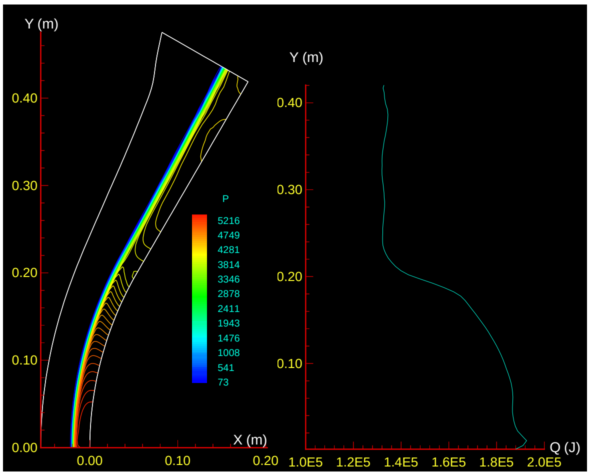

Figure 8: On the left, pressure flow-field during entry around INTERMARSNET; on the right, convective heat-flux over the geometry [24].

As other example, ***Figure 7*** shows the flow-field of diatomic oxygen outside and inside the ATV during its re-entry in presence of a fissure. This study [8] was undertaken to assess with a refined approach the risk of explosion at high altitude at the end of the mission. The typical re-entry CFD simulation for prediction flow-field and heat-flux is displayed in ***Figure 8*** where the pressure flow-field and the heat-flux distribution for the INTERMARSNET probe during its Mars entry are displayed.

6. RADIATION

Depending en entry conditions and planet atmosphere, radiation has to be investigated. The radiation code PARADE [20-21] is available for this objective. This software computes the plasma emission and absorption. It relies presently on the assumption of Boltzmann equilibrium for the excited states distributions. Its database, initially limited to air species, has been extended to carbon species such as C, CN and CO. Though also usable for the prediction or rebuilding of experimental spectra, the primary goal of PARADE is the calculation of the radiative heat flux at the wall of an entry vehicle. Simplified one-dimensional transfer models have been included into the software, to provide a quick assessment of the flux. The code can be interfaced with TINA or PMSSR to provide one dimensional coupled solutions.

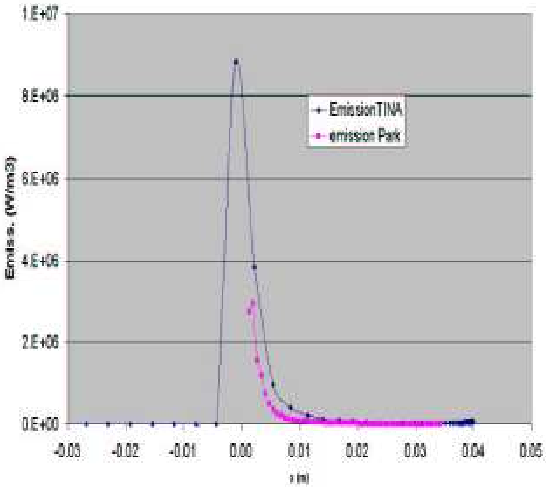

Figure 9: Emitted radiative power along the stagnation line for the thermochemical models of TINA and Park [26] and a Mars atmosphere.

This code has been used to evaluate the radiation level for a Mars entry [25] in the frame of the activities performed for the ESA Radiation Working Group. This study has shown that the presence of nitrogen in the Mars atmosphere has to be accounted for. A large sensitivity of radiation to the thermochemical model has been shown. The computations made with the chemistry models of Park [24] and TINA provided different levels of radiative emission as shown in ***Figure 9***. The discrepancy has been attributed to the large differences in temperature evolutions for the different simulations. The two models provided similar vibrational temperature profiles and CO number density distributions. However, TINA results were corresponding to a slightly larger, hotter shock layer, producing a large and narrow peak of radiative emission. The differences in shock stand-off distance also contribute to the result dispersion. A detailed review of the thermo-chemistry models for a Mars atmosphere will be necessary to close this point and to improve the reliability of the radiation predictions.

7. ABLATION

Most of the thermal protection systems are made of ablative material. Ablation has a strong impact on heat-flux and the prediction of material recession is necessary for sizing the TPS. Heat-shield recession calculations can be performed using FABL [27] and KCMA [28] two software based on a one dimensional approach. The prediction on heat-flux accounting for ablation can be achieved using TINA and a blowing condition at the surface. The differences between ablative and non ablative numerical simulation can be seen in ***Figure 10***, representing the temperature contours around a capsule with and without ablation. The numerical simulations [24] have been performed for a high speed Earth entry typical of a sample return mission with an entry velocity of 14 km/s. For the ablative computations the thermal protection system was supposed to be in carbon phenolic. The temperature flow-field shows that the presence of ablation has for effect to cool down the shock layer.

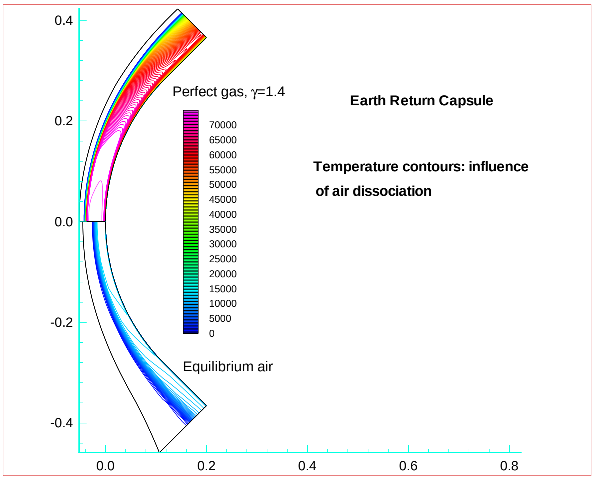

Figure 10: Temperature contours around the EURORETURN capsule with (bottom) and without ablation (top) for an entry velocity of 14 km/s.

8. CONCLUSION

Through the different software available at ISA and the experience acquired in several projects the modelling of the different flow phenomena characterizing a re-entry can be performed. Existing tools cover the flow regimes from rarefied to supersonic and incompressible flows. Some software are based on engineering approaches, others are more sophisticated and solve Navier-Stokes, Boltzmann or Maxwell equations, some tools are more oriented to system studies related to the generation of aerodynamic database or re-entry aerothermodynamics.

Efforts are actually made in the domain of blackout for IRDT post-flight analysis and ablation with a study on convective blockage for high-speed Earth entry. This will bring new developments in the existing tools and will increase their capabilities and their accuracy for the prediction of heat-flux level, ablation recession and blackout during entries into planet atmospheres.

The author of this paper thanks Dr L. Marraffa from ESA-ESTEC and A. Smith from FGE for their comments and support.

9. REFERENCES

1. Smith A., J. & Parnaby G., "Program TRAJ3D V2.2 three degree of freedom planetary entry and descent trajectory simulation user manual", TN 133/92 Issue 7, Fluid Gravity Engineering, March 2003.
2. Daley, S., A six degree of freedom trajectory prediction model: Program TRAJ6DA Version 3, TN22/95, Issue 3, Fluid Gravity Engineering, Feb. 2005.
3. Schneider, D. Z., CREAM V1.0, CR048/05, Fluid Gravity Engineering, August 2005.
4. Smith, A. J., RKHMP-19 User Guide, TN157/94 Issue 3, Fluid Gravity Engineering, June 1998.
5. Reynier, Ph., & Marraffa, L., Aerothermodynamics investigations for Earth orbital entry vehicles, In *Proceedings of 4th International Symposium on Atmospheric Reentry Vehicles and Systems*, Arcachon, March 21-23, 2005.
6. Marraffa, L., Mazoué, F., Reynier, Ph., & Reimers, C., Some Aerothermodynamics Aspects of ESA entry probes, *Chinese Journal of Aeronautics*, Vol. 19(2), pp. 84-91, May 2006.
7. Babakin Space Center, "IRDT-2RE-Flight Mission: Summary Analysis Report", BSC-IRDT2R-SAR-0001, Babakin Space Center, Moscow, Nov. 2003.
8. Boutamine, D. E., Reynier, Ph., Schmehl, R., Steelant, J. & Marraffa, L., Computational Analysis of ATV Re-entry Flow and Explosion Assessment, ESA Working Paper, E.W.P. 2304, Jan. 2006.
9. Reynier, Ph., & Mazoué, F., PARES: Trajectory Analysis, Internal Note (ESA-PARES-TN-05-05-rev2), ESA/ESTEC, June 2005.
10. Reda D. C., Correlation of nosetip boundary-layer transition data measured in ballistics range experiments, *AIAA Journal*, Vol. 19(3), pp. 329-339, 198.
11. Parnaby G. & White T., Transition in hypersonic boundary layers – Literature survey, CR035/03, Fluid Gravity Engineering, July 2003.
12. Morabito D. D., The spacecraft communications blackout problem encountered during passage or entry of planetary atmospheres, IPN Progress Report 42-150, Jet Propulsion Laboratory, 2003.
13. Dubois, J., & Smith, A. J., "Program PMSSR V4.1: Inverse shock layer solution with non-equilibrium thermochemistry", TN 132/92-Issue 3, Fluid Gravity Engineering, Aug. 2004.
14. Aerocapture: Technology Demonstrator, CDT Study Report 21(A), ESA-ESTEC, Nov. 2004.
15. Dunn, M. G., Comparison between predicted and measured blackout boundaries for Earth entry of Apollo, NASA Technical Report 71N21104, Jan. 1970.
16. Smith, A. J., Bell, D., & Boulton, D., "TINA Version 4: Theory and User Manual", TN 89/96 Issue 4, Fluid Gravity Engineering, 2002.
17. Smith, A. J., ESA PlasmA Radiation DatabasE (PARADE). Development, History, Status, Current developments and Future Prospects, *ESA-SP-533, Proceedings of the 1st International Workshop on Radiation of High Temperature Gases in Atmospheric Entry*, Lisbon, Oct. 8-10, 2003.
18. Pfeiffer, B., Fertig, M., Winter, M., & Auweter Kurtz, M., PARADE a program to calculate the radiation of atmospheric re-entry in different atmospheres, *ESA-SP-533, Proceedings of the 1st International Workshop on Radiation of High Temperature Gases in Atmospheric Entry*, Lisbon, Oct. 8-10, 2003.
19. Reynier, Ph., Modélisation d'écoulements complexes pour des applications aérospatiales, Habilitation à Diriger les Recherches, Université Bordeaux 1, In preparation.
20. Gerhold, T., Friedrich, O., Evans, J., & Galle, M., Calculation of complex three dimensional configurations employing the DLR TAU code, AIAA Paper, 97-0167, 1997.
21. Rist, U., Instability and transition mechanisms in laminar separation bubbles, *Lecture Series on Low Reynolds Number Aerodynamics on Aircraft*, Von Karman Institute, 2003.
22. Radespiel, R., Numerical simulation of laminar separation bubbles, *Lecture Series on Low Reynolds Number Aerodynamics on Aircraft*, Von Karman Institute, 2003.
23. Barkley, D., Gomes, M. G. M., & Henderson, R. D., Three-dimensional instability in flow over a backward-facing step, *Journal of Fluid Mechanics*, Vol. 473, pp. 167-190, 2002.
24. Reynier, Ph., Marieu, V., & Marraffa, L., Aerothermodynamics Developments for Planetary Missions, *In Proceedings of 1st Joint French-German Symposium on Simulation of Atmospheric Entries by Means of Ground Test Facilities, SSAE 99*, pp. 2.5.1-2.5.8, Stuttgart, Nov. 17-19, 1999.
25. Reynier, Ph., Lino da Silva, M., Marraffa, L., & Mazoué, F., Preliminary study of Mars entry: Application to the prediction of radiation, *ESA-SP-533, Proceedings of 2nd International Radiation Workshop*, Porquerolles, France, Oct. 1-2, 2004.
26. Park, C., *Nonequilibrium Hypersonic Aero-thermodynamics*, John Wiley & Sons Inc., New-York, 1989.
27. Smith, A. J., FABL3, a program for analysing charring ablation thermal protection systems, TN20/96 Issue 3, Fluid Gravity Engineering, May 2000.
28. Ahn, H.-K., Park, C., & Sawada, K., Response of Heatshield Material at Stagnation Point of Pioneer-Venus Probes, *Journal of Thermophysics and Heat Transfer*, Vol. 16, pp. 432-439, 2002.